Hydraulic and mass transfer performances of a commercial hybrid packing: the RSP200X -Key modelling parameters for gas treatment applications

Pascal Alix, John Roesler, Xavier Courtial, Michael Schultes

Hydraulic and mass transfer performances of a commercial hybrid packing: the RSP200X - Key modelling parameters for gas treatment applications.

Pascal Alix[a *], John Roesler[a], Xavier Courtial[b], Michael Schultes[c]

[a]IFP Energies nouvelles, BP 3, 69360 Solaize, FRANCE
[b]AXENS 89, Bd Franklin Roosevelt – 92500 Rueil-Malmaison - France
[c]RASCHIG GmbH, Mundenheimer Straße 100, D-67061 Ludwigshafen, GERMANY

The RSP200X , as one of the latest generation of Raschig's structured packings (Raschig Super-Pak ,RSP), has been investigated for use in scrubbing columns operating at high liquid loads where it could be particularly well adapted. These RSP packings offer a good potential for increasing capacity while maintaining mass transfer efficiencies at high levels. IFPEN has measured hydraulic and mass transfer performances in two columns of different diameters (146 mm and 1000 mm). Flooding limits were in agreement with literature, however at high liquid loads and for the tested X-Style RSP they were 30-40% lower than those calculated with the Winsorp Software delivered by Raschig. With the support of the present results a modified version of Winsorp has been elaborated for high liquid loads and X-Style RSP. In terms of mass transfer, the CO_2/MDEA system was used to measure $k_L a_e$ while the classic CO_2/NaOH and SO_2/NaOH systems were used for a_e and $k_G a_e$ measurements. The RSP200X was found to develop a high interfacial area compared to its geometric area. While for standard packings the gas flow rate is often considered to have only a small effect on effective area when operating below the loading point, its effect measured on RSP200X is significant and of the same order as for liquid load. Measurements of $k_L a$ and $k_G a$ further confirm these trends.

Keywords : hybrid structured packing, characterization, mass transfer, pressure drop, Raschig Super Pak, RSP.

1. Introduction

The latest generation of Raschig's structured packings RSP (Raschig Super-Pak) can be considered for scrubbing columns operating at high liquid loads to increase hydraulic capacity while maintaining intensive mass transfer efficiencies. This translates into design optimization since it could minimize column diameter and packed bed height for fixed liquid and gas flowrates, and fixed specifications of the treated gas. RSP packings have a specific geometry that is significantly distinct from standard high capacity structured packings as they present large openings all along corrugated metal sheets (figure 1). This geometric structure gives them features of simultaneously random and structured packings, hence they are are commonly referred to as hybrid packings. The RSP200X (Schultes, 2017) is a relevant case study among RSP series, since it can handle a wide range of liquid loads (from 10 to higher than 120 $m^3/m^2/h$) and develops an effective area close to those of earlier structured packings with geometrical areas of 250 m^2/m^3 .

Experiments have been conducted in two different columns with diameters of 146 and 1000 mm to measure hydraulic and mass transfer performances in terms of pressure drop, flooding limits, interfacial area and liquid and gas side mass transfer coefficients of the RSP200X. The results illustrate the performances of this hybrid packing, and highlights the need to consider the effect of gas flowrate on mass transfer rates unlike for standard structured packings.

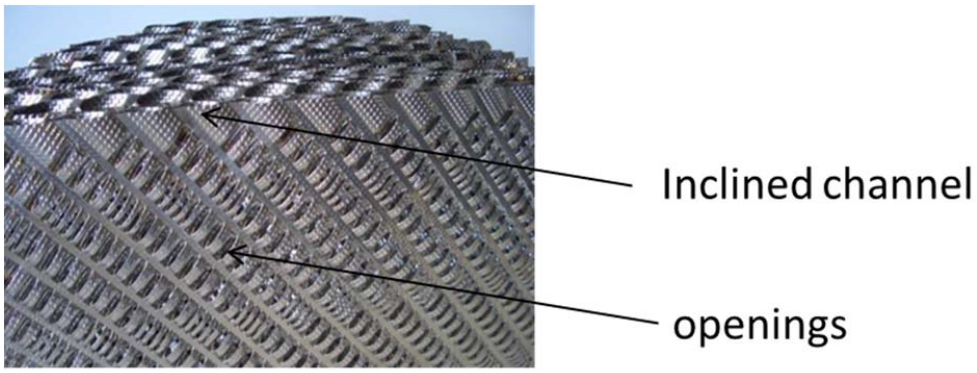

Figure 1 : Side view of a RSP structured packing.

2. Experimental facilities / methods

Two test columns available at IFPEN premises in Solaize (France) have been used for this work. The first one is a 146 mm inner diameter stainless steel column with a 3 meter bed height. It operates at room temperature and pressures from 1.2 to 2 bar abs. Liquid loads, Q_L, of 200 $m^3/m^2/h$, and gas load factors, F_s, of 5 $Pa^{0,5}$ can be reached if needed. This first column will be called D146 in this manuscript. The second one is a 1000 mm inner diameter transparent column with a 3 meter bed height. It operates at room temperature and pressure. Liquid loads of 100 $m^3/m^2/h$, and gas load factors of 4 $Pa^{0,5}$ can be reached if needed. This second column will be called D1000 in this manuscript.

Measurements in both columns have been performed with similar protocols when possible. Hydraulic parameters (pressure drop, flooding limits) have been measured with the air/water system. The global effective area, a_{eg}, has been measured with the absorption of CO_2 from air into a solution of NaOH at 0,1N, which leads to a pseudo-first order fast chemical reaction in the liquid phase (Wang, 2015, Hoffmann et al., 2007). Since CO_2 concentrations are very low, around 400 ppm, its absorption affects neither the liquid properties nor the superficial gas velocity, V_{SG}, which are considered constant. The value of a_e is thus given by :

$$a_{eg} = \frac{1}{H} \times ln\left(\frac{y_{CO2,out}}{y_{CO2,in}}\right) \times \frac{He \times V_{SG}}{RT \times \sqrt{k_{cin} \times D_{CO2,L}}}$$

This value represents the global effective area and includes the contribution from the column walls. Assuming all wall surfaces are wetted they contribute 4/D to the measured value. In the D146 column this represents 27.4 m^2/m^3 but only 4 m^2/m^3 in the D1000. The packing effective area is then evaluated as

$$a_e = a_{eg} - 4/D$$

The kinetic constant, k_{cin}, Henry constant, He and liquid diffusion coefficient, D_L, are calculated following the work of Pohorecki and Moniuk (1987). The molar fractions of CO_2, y_{CO2}, are measured with an infra-red on-line analyser which is calibrated daily.

Liquid side mass transfer coefficients, $k_L a_e$, are measured by absorption of CO_2 diluted with air into a 3-4%wt MDEA solution. This system leads to a slow chemical reaction when the CO_2 loading, α_{CO2}, is above 0.08 and is only mildly sensitive to thermodynamic and kinetic uncertainties when the loading stays below 0.22 (Roesler et al., 2016 & 2018). The gas phase inlet CO_2 molar fraction used in the large D1000 column is around 0.25%, and around 0.9% in the D146 column. With these mixture compositions and with only about 10 to 15% of the injected CO_2 absorbed along the column, the liquid properties and V_{SG} can be considered constant. The $k_L a_e$ is thus given by :

$$\begin{cases} Ek_L a_e = \dfrac{He \times V_{SG}}{RT \times H} ln\left(\dfrac{y_{CO2,in} - {y_{CO2}}^*}{y_{CO2,out} - {y_{CO2}}^*}\right) \\ {y_{CO2}}^* = \dfrac{He}{P} \times C_{CO2,bulk} \end{cases}$$

With

$$\begin{cases} E = \dfrac{Ha}{th(Ha)} \\ Ha = \dfrac{\sqrt{(k_{cin} D_{L,CO2})}}{k_L} \end{cases}$$

The values of CO_2 concentration in the liquid bulk, $C_{CO2,bulk}$, CO_2 Henry's constant, He, and the enhancement factor, E, are calculated with an in-house simulator. The range of values of the parameters that impact the calculation of $k_L a_e$ for the present experiments are specified in Table 1.

Table 1 : Ranges of parameters for $k_L a_e$ calculations.

Parameter	Min Value	Max value
C_{MDEA} (%wt)	3.3	3.5
α_{CO2} (mol CO_2 / mol MDEA)	0.11	0.16
T (°C)	22	25
He (Pa/(mol/m^3))	2620	2837
$y_{CO2}{}^*$	3.5x10^{-4}	8.8x10^{-4}
$k_{cin}D_{L,CO2}$ (m^2/s^2)	8.6x10^{-10}	9.9x10^{-10}
E	1.01	1.04

Provided the calculation of $y_{CO2}{}^*$ is accurate, the partial pressure of CO_2 should not impact the $k_L a_e$ evaluated for fixed operating conditions. Figure 2 gives the $k_L a_e$ determined in the D146 facility as a function of the partial pressure of CO_2, P_{CO2}, at fixed α_{CO2} of 0.15 and 0.07. The $k_L a_e$ are constant between 0.1 kPa and 2 kPa, which corresponds to our present experimental range (~0.25 kPa for D1000, ~1.35 kPa for D146. The black symbols show the full calculation while the white squares show the values obtained if $y_{CO2}{}^*$ is neglected for the loading case of 0.15. The results show that equilibrium considerations are secondary at 1 kPa of CO_2 and can almost be neglected, whereas they must be taken into account at lower partial pressure (0.2 kPa). Since all black symbols give the same $k_L a_e$ within measurement uncertainties, our thermodynamic model properly evaluates the value of $y_{CO2}{}^*$ within the range of values given in Table 1.

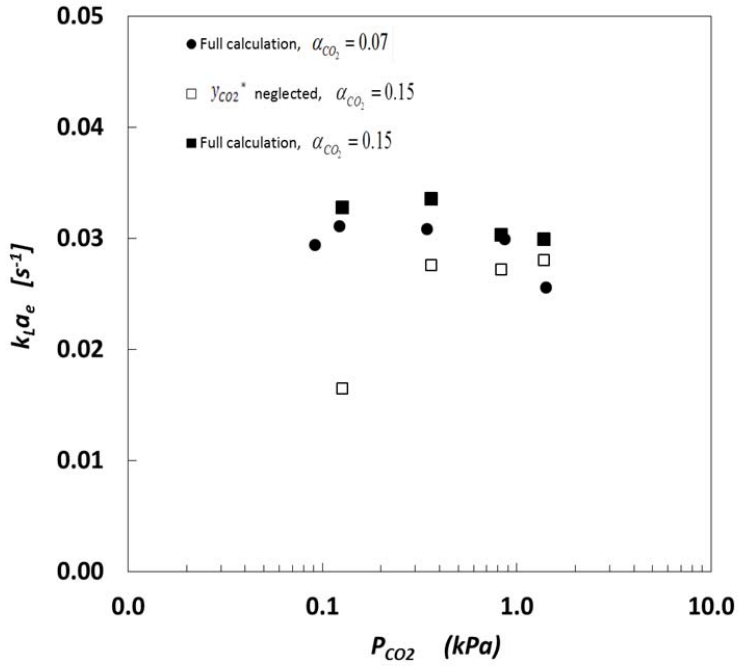

Figure 2 : Experimental $k_L a_e$ as a function of CO_2 partial pressure, D146, MDEA 3.2%. α_{CO2}=0.07 and 0.15 ; Q_L=70 m^3/m^2/h ; F_s=0.32 Pa$^{0.5}$.

Figure 3 gives the calculated *E* as a function of the k_L using a representative value of 9.25×10^{-10} m^2/s^2 for $k_{cin}D_{L,CO2.}$ The present method is well adapted for k_L>2.10^{-4} m/s since enhancement factors are then close to 1. When k_L<3.10^{-5} m/s, the present method is less well adapted since kinetics plays a significant role (more than 20%). In between, which is our experimental range, the impact of the reaction rate on the absorbed rate is less than 10%. The present method is still nicely adapted and the user can take into account the enhancement factor to improve the accuracy of the measurements. When $k_{cin}D_{L,CO2}$ and y_{CO2}^* are considered this CO_2/MDEA system gives results similar to those obtained with O_2 desorption from water into air or nitrogen. It should be noted that this reactive absorption system is complementary to physical desorption methods in the sense that it is well adapted to tall beds (Roesler *et al*., 2018) where desorption systems might reach equilibrium limitations. The CO_2/MDEA system is used by default at IFPEN to measure $k_L a_e$, If operating conditions are not adapted then O_2 absorption or desorption is used.

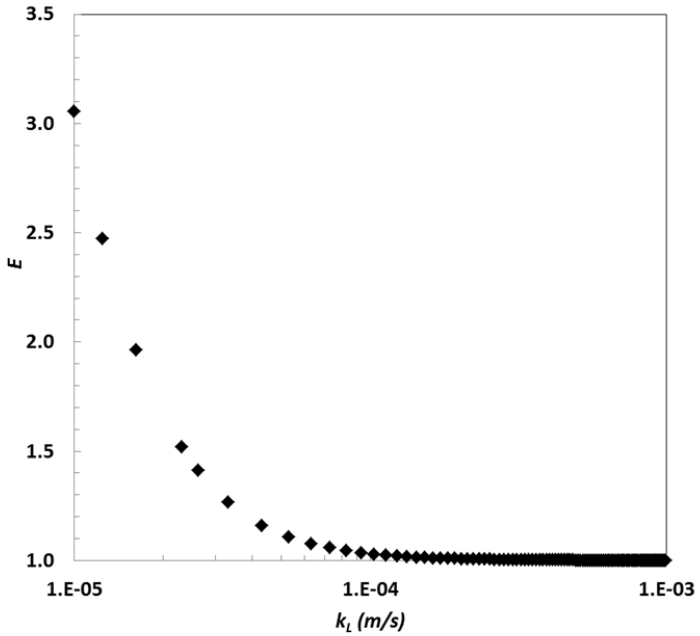

Figure 3 : Calculated E as a function of k_L for the CO_2/MDEA system.

Gas side mass transfer coefficient, $k_G a_e$, were determined in the D146 column only by measuring the absorption rate of SO_2 diluted with air into NaOH (2N) (Hoffmann et al., 2007) which leads to an instantaneous chemical reaction. Since the molar fraction of SO_2 in the gas phase is low (3 000 < $y_{SO2,in}$ < 11 000 ppm), its absorption changes neither the gas velocity nor the liquid properties. The $k_G a_e$ is then given by:

$$k_G a_e = \frac{V_{SG}}{RT} \times \frac{1}{H} \times ln\left(\frac{y_{SO2,in}}{y_{SO2,out}}\right)$$

For $k_G a_e$ measurements, the bed height is reduced to 2 packing blocks (about 0.4 m), and a liquid pre-distributor is used to minimise entrance effect (figure 4). The pre-distributor is a single 100 mm thick plastic block of IS4D packing (Alix *et al.*, 2011). The experimental protocol accounts for the end effects of the setup t. The latter are subtracted out in the calculation based on measurements made with and without packing to obtain a net $k_G a_e$:.:

$$(k_G a_e)_{net} = \frac{(H + H_{IS4D}) \times (k_G a_e)_{tot} - H_{IS4D} \times (k_G a_e)_{ref}}{H}$$

For all measurements, gas and liquid concentrations are measured at column inlet and outlet

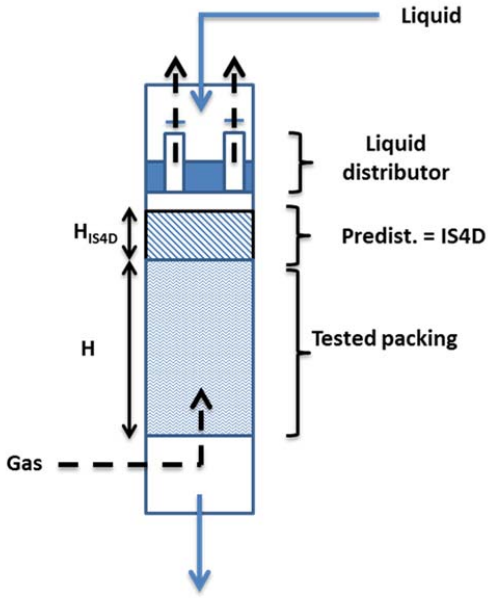

Figure 4 : Schematic of the D146 column for $k_G a_e$ measurements.

3. Hydraulic performances

Pressure drop and flooding limits were measured for Q_L from 10 to120 $m^3/m^2/h$ and compared to both the results of Wang (2015) and the calculations from two versions of the Raschig software: “Winsorp” and “Winsorp 2017”. The latter version is a recent update that incorporates results from this work. Wang used a bed height of 3.05 m in a 430mm inner diameter column that will be referred to as D430. As shown in Figure 5 for Q_L =60 $m^3/m^2/h$, IFPEN and Wang results are in good agreement. The D146 results are only slightly staggered which indicates that there is no major effect of diameter on the present measurements. However, a clear discrepancy is apparent between the data and the calculations from the Winsorp software which over predict flooding limits by 30-40%. Investigations with Raschig showed that the hydraulic model in the software was based on distillation tests performed at low liquid loads only. The IFPEN tests have explored the higher loading rates and indicate that extrapolation of flooding models should be used with caution to size column diameters for fluid systems and liquid loads that differ from those from which these models were based on. With the support of the new results, a modified version of the software, “Winsorp 2017”, has been elaborated for high liquid loads and X-style RSP.As shown in Figure 5 the modified version now closely follows the data. Similar conclusions are reached at a higher liquid load of100 $m^3/m^2/h$ as shown in Figure 5b. The mean absolute relative error is lower than 10% for the new version, which is similar to the experiments’ reproducibility.

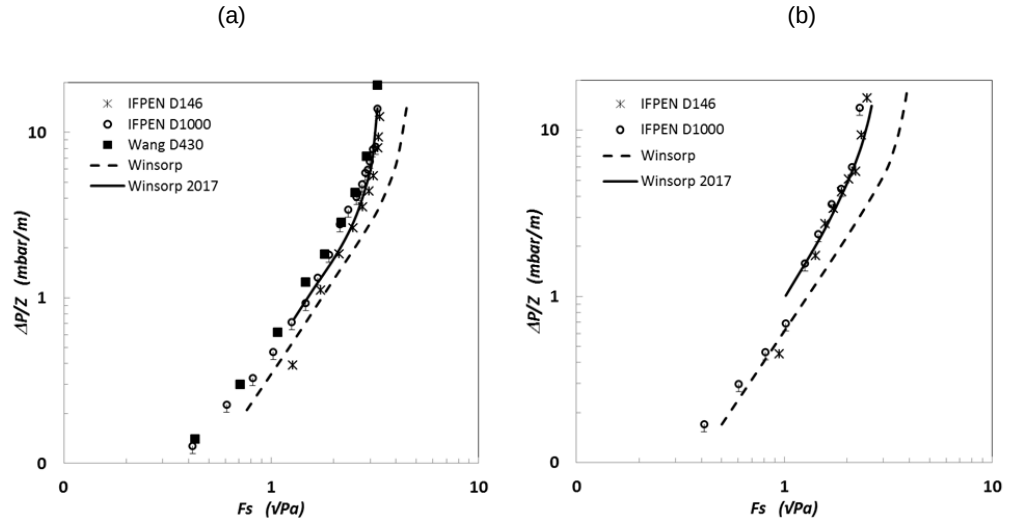

Figure 5 : Pressure drop of the RSP200X. Comparison of IFPEN measurements on D146 and D1000, with results of Wang (2015) on D430, and calculations of both Winsorp versions (original and revised in 2017). For Q_L=60 $m^3/m^2/h$ (a) and Q_L=100 $m^3/m^2/h$ (b).

4. Mass transfer performances

The experiments conducted at IFPEN served to characterize the mass transfer parameters of RSP200X in terms of effective interfacial area and mass transfer coefficients both on the liquid and gas sides .

4.1 Effective area : a_e

Figure 6 gives the ratio of effective areas measured by IFPEN relative to those of Wang (2015, D430), as a function of the ratio Q_L /$Q_{L,ref}$ for low F_s around 0.6 and high F_s between 1.5 and 2 $Pa^{0,5}$. From a global perspective, since the reported ratios fall between 0.8 and 1, the areas measured in the three columns agree within the typical experimental uncertainties of 20% for this method of measurement (Hoffmann et al., 2007). The impact of Q_L is similar in all columns since the ratios show little variation. The impact of F_s seems to be a bit different in the D146 since the ratios of effective areas decrease at higher F_s. This could be linked to the ratio of the column to hydraulic diameter of the packing (close to 20mm for the RSP200X) which equals 7.3 for the D146. This value is lower than the one recommended by Olujic (1999) to eliminate size effects. IFPEN values measured with D1000 are systematically lower than those of Wang. Here the difference with the results of Wang is probably not the consequence of a diameter effect since the ratio of the column diameters to hydraulic diameter are well above 7.3, equalling 50 in the D1000 and 21.5 in the D430. The difference cannot be attributed to the reactive absorption model since the thermodynamic and kinetic sub-models used are identical. Effects related to the liquid distributor (Wang uses a fractal liquid distributor) or to a difference in the temperature used for the chemical reaction rate are the most probable causes.

For a fixed Q_L of 60 $m^3/m^2/h$, Figure 7 gives the ratio $a_e/a_{e,ref}$ as a function of the ratio $F_s/F_{s,ref}$ for both IFPEN and Wang (2015) results, where $a_{e,ref}$ is the effective area measured at F_s = $F_{s,ref}$ =0.65 $Pa^{0,5}$. Figure 7 shows that the gas load impacts the effective area for the D430 and D1000 columns, a_e could be increased by 20% (solid line). This was not expected since it cannot be explained by the hydraulics regime: the loading point is reached at F_s = 2.3 $Pa^{0,5}$ for this liquid load (see Figure 5). Again, the behaviour of the D146 is a little bit different; gas load effect is lower and not significant below a ratio of 2. This specific point has been explained by a moderate diameter effect. The impact of the gas load on the effective area has been observe for some random packings (Wang et al., 2005), however it is not common for structured packings. Hybrid packings like RSP200X are considered between random and structured packings, this could explain present results. This seems to indicate that, for some hybrid packings, an effect of the gas load should be considered to improve the accuracy of correlative models of mass transfer parameters.

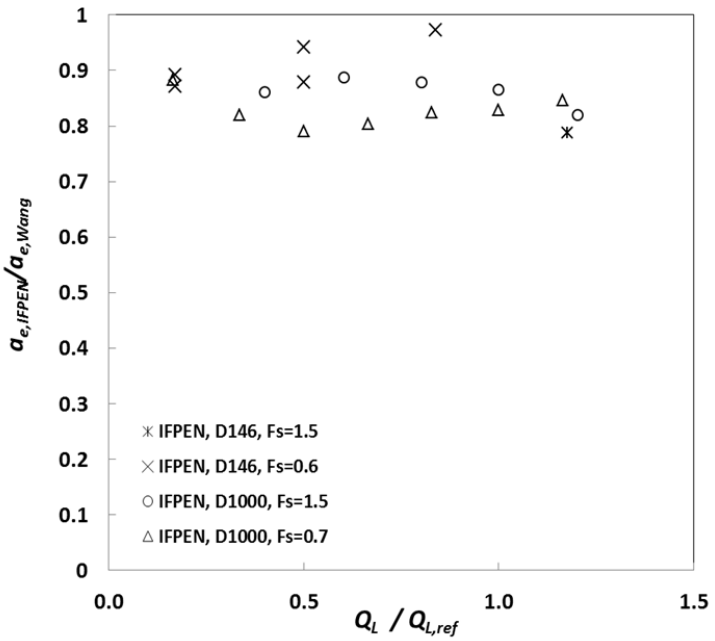

Figure 6 : Effective areas measured by IFPEN (with D1000 and D146) and by Wang (2015) on the D430 as a function of the ratio Q_L /$Q_{L,ref}$, at F_s = 0.6 - 2 $Pa^{0,5}$. $Q_{L,ref}$ =60 $m^3/m^2/h$.

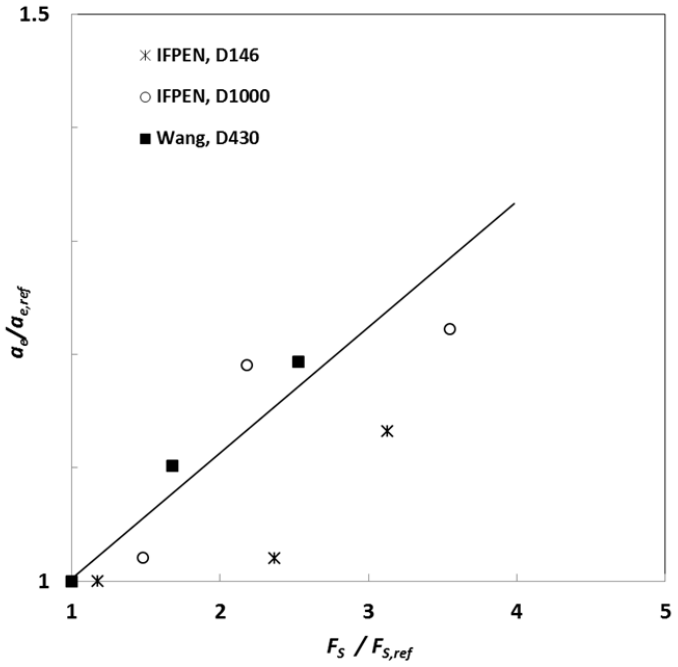

Figure 7 : Ratio of measured effective area to the one measured at $F_{s,ref}$ = 0.65 $Pa^{0,5}$, as a function of $F_s/F_{s,ref}$ at a fixed liquid load of Q_L=60 $m^3/m^2/h$ for IFPEN and Wang (2015) results.

4.2 Liquid side mass transfer : k_La_e

Figure 8 gives k_La_e values measured by IFPEN as a function of the ratio Q_L /$Q_{L,ref}$, at F_s = 1.5 $Pa^{0,5}$ and for $Q_{L,ref}$ =60 $m^3/m^2/h$. Measurements are compared to those of Wang (2015). First, it should be noted that Wang uses the physical desorption of Toluene from water to measure k_La_e. Therefore to compare results, the raw data from Wang needs to be corrected in order to represent the transfer rate of CO_2 in a dilute MDEA solution as used in the IFPEN measurements. For that purpose, the raw data are multiplied by the ratio of the square root of the liquid diffusivities of Toluene and CO_2 into water, since the impact of the MDEA at 3%wt is negligible. Figure 8 shows that IFPEN and Wang measurements are in reasonable agreement. On the other hand, the values from the D146 column are significantly lower than those from D430 and D1000 columns. This confirms the existence of a significant diameter effect on the liquid phase, whereas only moderate size effects are seen on hydraulic and effective area measurements.

Figure 9 gives the ratio of the experimental k_La_e to the one measured at $F_{s,ref}$ = 0.5 $Pa^{0,5}$, as a function of ratio $F_s/F_{s,ref}$. The reference liquid load is fixed, Q_L =60 $m^3/m^2/h$. D1000 results have been selected since those from D146 are impacted by the column walls. A gas load effect is clearly shown in Figure 9 where k_La_e increases by more than 20% for $F_s/F_{s,ref}$ = 3. This variation is similar to the one observed for the effective area and confirms the need to consider a higher than usual gas load effect on effective area for hybrid structured packings.

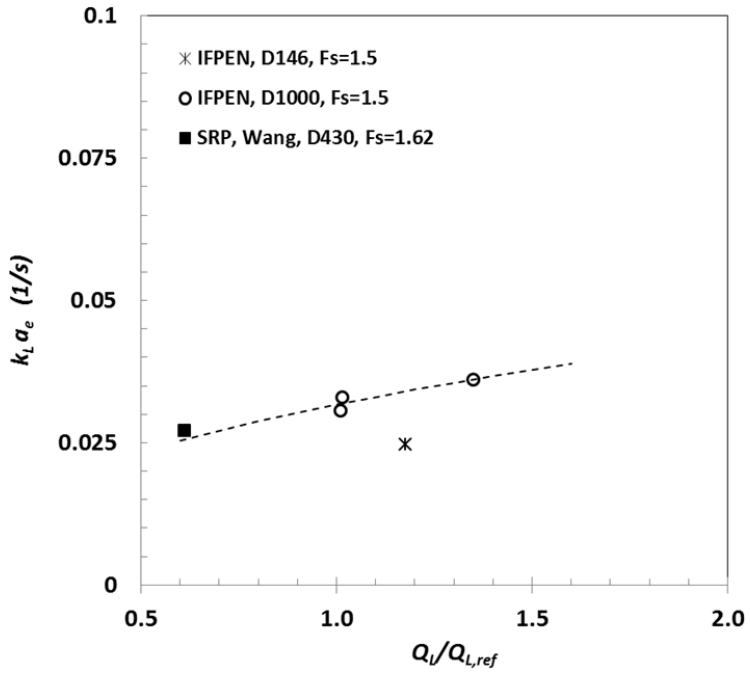

Figure 8 : k_La_e as a function of the ratio Q_L /$Q_{L,ref}$, at F_s = 1.5 $Pa^{0,5}$. IFPEN measurements vs. Wang "corrected" measurements. $Q_{L,ref}$ =60 $m^3/m^2/h$.

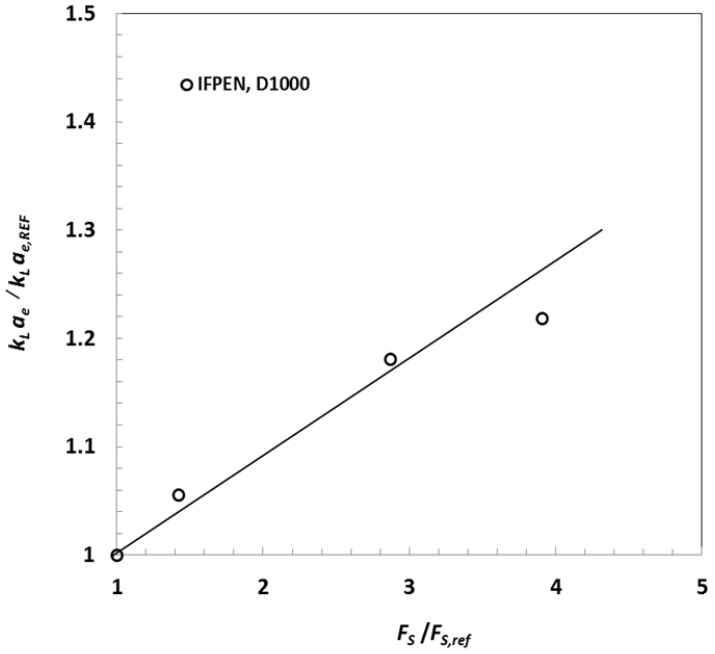

Figure 9 : Ratio of $k_L a_e$ with the one measured at $F_{s,ref}$ = 0.5 $Pa^{0,5}$, as a function of $F_s/F_{s,ref}$ and at Q_L=60 $m^3/m^2/h$. IFPEN measurements (D1000).

4.3 Gas side mass transfer : $k_G a_e$

The $k_G a_e$ values have been measured in the D146 column (*cf*. 2.). The IFPEN column is operated at an absolute pressure around 2 bar while the Wang column (2015) operates at atmospheric pressure. With these pressure differences, k_G values cannot be compared directly. The Sherwood number should be used as it considers the impact of the gas diffusivity, $D_{G,SO2}$:

$$Sh_G = \frac{k_G d_{eq}}{D_{G,SO2}} \tag{1}$$

For the present structured packing:

$$d_{eq} = \frac{4}{a_g} \tag{2}$$

where a_g is the geometric specific area of the RSP200X, which is equal to 200 m^2/m^3. It must be noted that IFPEN k_G values have been calculated by dividing $k_G a_e$ with interfacial areas measured in the D146 column in order to be coherent with the $k_G a$ values.

Figure 10 displays the Sherwood number as a function of the gas Reynolds number, and compares IFPEN values to those of Wang (2015). The gas Reynolds number takes into account the impact of the pressure on the hydraulics:

$$Re_G = \frac{\sqrt{\rho_G} F_S d_{eq}}{\mu_G} \tag{3}$$

where μ_G is the gas dynamic viscosity (Pa.s), and ρ_G is the gas density (kg/m^3). The IFPEN measurements are observed to be in good agreement with Wang measurements. This indicates that there is a negligible diameter effect on k_G unlike for the k_L (see 4.2). The present measurements could therefore be used to build correlations for bigger

columns. At Re_G=3000, the Wang value is not in line with other ones and seems to be too low. This could be explained by the fact that at such high gas flowrates the SO_2 concentrations in the gas leaving the packed bed become very low such as to generate higher experimental errors. Upon extrapolation to the intercept, the Sherwood number follows a power law dependency of 0.83 relative to the gas Reynolds number, which is in agreement with a majority of publications that recommend 0.8 (Wang et al., 2005). This also confirms the fact that there is no significant diameter effect on the present results.

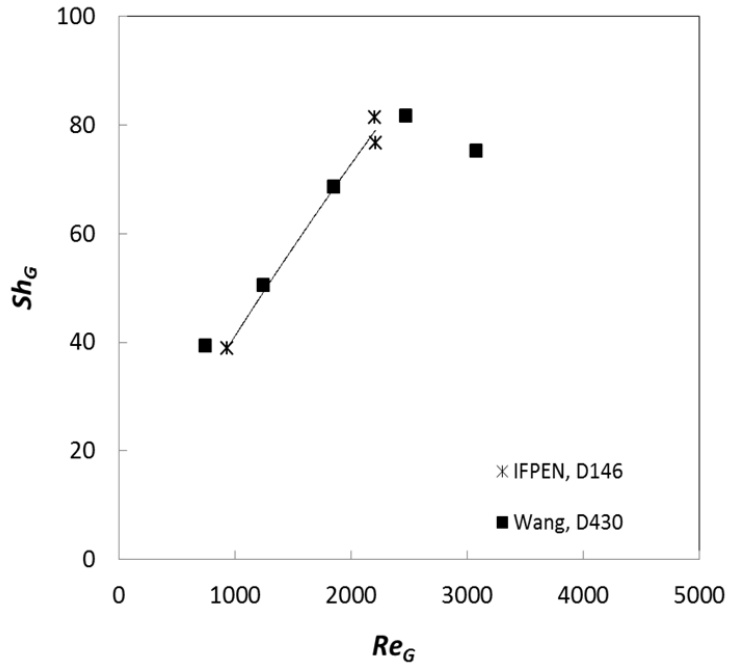

Figure 10 : Gas Sherwood number as a function of the gas Reynolds number. IFPEN measurements (D146) vs. Wang measurements (D430, 2015), at Q_L=30-70 $m^3/m^2/h$.

5. Conclusions

Experiments with the RSP200X Raschig hybrid structured packing have been performed in two test facilities with respective inner diameters of 146 and 1000mm. Pressure drop, flooding limits, and mass transfer parameters have been measured with model fluid systems. Of particular interest is the use of the CO_2/MDEA system for k_La_e measurement as it can be used in conjunction with large structured packing bed heights of 3 m and above, in contrast with common systems using physical absorption which are typically more limited in bed height due to saturation effects. The MDEA solutions must be pre-loaded in order to operate in the required slow reaction regime, and considerations for the CO_2 concentration in the liquid bulk and for the enhancement factor are needed to estimate k_La_e with good accuracy.

Hydraulic tests show that extrapolation of available flooding models should be used with caution to size column that use fluid systems and liquid loads different from those with which these models were derived. With the support of present results, a modified version of Winsorp (“2017”) has been elaborated by Raschig for high liquid loads and X-style RSP.

Mass transfer tests show that a gas velocity effect on interfacial area should be considered for hybrid packings like the RSP, which was an unexpected result for a structured packing. The k_La_e measurements also show an effect of the gas velocity that is largely related to the effective area changes. Column wall effects are highlighted in the D146

column, with consequences mainly on the liquid phase for the determination of k_L and to a lesser extent on a_e For the gas phase (k_G) this diameter effect is negligible. Finally, the present test results are in good agreement with those of Wang obtained in a 430 mm inner diameter column using a different chemical system to determine $k_L a_e$.

References

Alix, P., Raynal, L., Abbe, F., Meyer, M., Prevost, M., Rouzineau, D. 2011. Mass transfer and hydrodynamic characteristics of new carbon carbon packing: Application to CO_2 post-combustion capture. Chem. Eng. Res. And Design, 89, 1658-1668.

Hoffmann, A., Mackowiak, JF., Gorak, A., Haas, M., Löning, JM., Runowski ,T., Hallenberger, K., 2007. Standardization of mass transfer measurements. A basis for the description of absorption processes, Chem Eng. Res. And Design, 85(A1), 40-49.

Olujic Z., 1999. Effect of column diameter on pressure drop of a corrugated sheet structured packing, TransIChemE, 77, 505-510.

Pohorecki, R., Moniuk, W, 1987.. Kinetics of reaction between carbon dioxide and hydroxyl ions in aqueous electrolyte solutions. Chem. Eng. Sci. 43(7), 1677-1684.

Roesler, J., Royon-Lebeaud, A., Alix, P., 2016. Liquid side mass transfer coefficient measurements in tall structured packing beds by reactive absorption with dilute MDEA solutions. Paper Presented at 2016 AIChE Annual Meeting, San Francisco, CA, USA, November 13-18, Paper n°8467941.

Roesler, J., Alix, P., Royon-Lebeaud, A., Valenz, L., Haidl, J., Rejl, F., 2018. Evaluation of the $k_L a$ of structured packings in small diameter columns – the key role of wall wipers. Chem. Eng. Transactions, 69, 49-54.

Schultes, M., 2017. Raschig Super Pak. A new packing structure with innovative advantages. Product Bulletin 501.

Wang, GQ., Yuan, XG., Yu, KT., 2005. Review of mass transfer correlations for packed columns, Ind. Eng. Chem. Res., 44, 8715-8729

Wang, C., 2015, Mass transfer coefficient and effective area of packing. Thesis manuscript, The University of Texas at Austin.